Available online at www.sciencedirect.com

ScienceDirect

Materials Today: Proceedings 00 (2018) 0000–0000

www.materialstoday.com/proceedings

BioM&M_2018

Single track deposition study of biodegradable Mg-rare earth alloy by micro laser metal wire deposition

Ali Gökhan Demir*

Department of Mechanical Engineering, Politecnico di Milano, Via La Masa 1, 20156 Milan, Italy

Abstract

The high reactivity of the material is one of the key issues in powder-based additive manufacturing of biodegradable Mg-alloys. In fact, the powder feedstock is highly inflammable and difficult to manage in laser powder-bed fusion and metal deposition. On the other hand, wire feedstock can provide an intrinsically safer solution for the purpose. However, the process should be developed for maintaining geometrical precision and deposition quality. In this work, micro laser metal wire deposition (μLMWD) of a biodegradable Mg-alloy with Dy as the main alloying element (Resoloy) is demonstrated. A flash-pumped Nd:YAG laser was used along with a custom-built wire feeder. Single-tracks were deposited and analysed for their geometrical attributes, microhardness, and deposition efficiency. The results were evaluated to determine the processability of the heat sensitive Mg-alloy with respect to an austenitic stainless steel with known processability. Despite a narrow processability window, single-track deposits were successfully produced. Micrometric feature resolution was maintained with crack and pore free deposits.

Selection and Peer-review under responsibility of 1st International Conference on Materials, Mimicking, Manufacturing from and for Bio Application (BioM&M).

Keywords: Additive manufacturing; biodegradable metals; Mg alloys; directed energy deposition

1. Introduction

The use of Mg alloys for biomedical applications has gained increased attention over the past decade. The high corrosion rate of these materials is considered as the main drawback for most of the mechanical applications regarding automotive, aviation, and aerospace fields. On the other hand, the same can be exploited as a biodegradability feature

* Corresponding author. Tel.: +39 02 2399 8590; fax: +39 02 2399 8585.
E-mail address: aligokhan.demir@polimi.it

Selection and Peer-review under responsibility of 1st International Conference on Materials, Mimicking, Manufacturing from and for Bio Application (BioM&M).

for bioimplant manufacturing. Mg plays a key role on the functioning of the human metabolism influencing growth factor effectiveness, co-regulating energy metabolism, cell proliferation, protein synthesis, onset of DNA synthesis [1]. Hence biocompatibility of these alloys is an almost intrinsic feature. Stents [2][3], orthopaedic implants [4], sutures, plates, and screws [1] are some of the biomedical implants that can be produced using biocompatible and biodegradable Mg alloys. The manufacturing methods employed to produce the final device has a critical impact on the biological and biodegradation performance of the implant. The Mg-alloys possess low deformability, which renders production raw materials used for the production of biodegradable implants such as minitubes, wires, and plates considerably difficult [3,5–7]. Laser based manufacturing methods are also often employed during the manufacturing of biomedical implants. Laser microcutting is the principal method used for producing cardiovascular stents, which is often followed by chemical etching and electropolishing steps. Laser welding is used to assemble wires and plates. Processing of Mg and its alloys with a laser beam generates further complexity due to the high reactivity of the material [8] and low melting and vaporization points [9]. Especially in laser welding, variations in alloy composition, crack and pore formation, undercut generation are common defects, which can reduce the performance of the biodegradable implant [10][11].

Metal additive manufacturing techniques have opened up several possibilities for biomedical implant design [12]. Customized implants fit for patient with tailored mechanical properties are some of the possibilities [13–15]. Most of these manufacturing techniques rely on the use of an energetic beam for melting a powder or wire precursor following a desired trajectory. Commonly a laser beam is used due to its high intensity, which provides high process resolution and full melting of the precursor. The use of directed energy deposition (DED) techniques with a Mg-alloy wire feedstock can essentially be a valid option, which has been treated sparingly in literature. This is commonly due to the reduced process resolution in terms of smallest dimensions of layer thickness and width achievable [16]. Indeed, DED techniques have found more interest in terms of higher deposition rates and increased material use efficiency in the literature for especially constructing larger components [17–19]. The process resolution depends on the size of the wire feedstock and the used energy source, which can be a plasma, an electric arc, a laser or an electron beam. Laser beams provide the flexibility of operating in ambient atmosphere as well as a high intensity beam. Several works are reported in the literature, where the deposit width is 5 to 15 times the wire diameter and the used wire diameter is around 1 mm [20–23]. More recently, the attention towards higher precision in metal wire deposition processes has emerged. Jhavar et al proposed a micro plasma transferred arc (μPTA) wire deposition process, where a 0.3 mm diameter AISI P20 tool steel, could be deposited with a track width of approximately 2 mm [24]. Further reduction of the feature size depends highly on the control over the energy deposition rate. From this point of view, the use pulsed wave (PW) lasers can provide the solution [25][26]. Demir [27] has demonstrated the use of a ms-long pulsed Nd:YAG laser for micro laser metal wire deposition (μLMWD). Thin-walled structures with 0.7 mm wall thickness and high aspect ratio were successfully deposited from a 0.5 mm AISI 301 wire. With confirmed feasibility of the approach, its extension to heat sensitive materials such as biodegradable Mg alloys is a natural consequence. As a matter of fact, metal wire deposition of Mg-alloys has received very little attention from the research communities.

Accordingly, this work evaluates the processing characteristics of a commercial biodegradable Mg-alloy with rare earth addition (Resoloy) by μLMWD. The first part of the work consists of a single-track deposition study revealing the processability window, the geometrical characteristics, microhardness and microstructure of the deposits obtained within. In the second part, an analytical model is employed to estimate the temperature gradients to better explain the limits in the processability. Comparisons with an austenitic stainless steel with known processability is made use of in order to better explain these limitations.

2. Experimental methods and materials

2.1. Material

A commercial Mg alloy with dysprosium as the main alloying element and a patented chemical composition was the used wire material (Resoloy, Fort Wayne Metals, Fort Wayne, Indiana, USA) [28]. Dy has high solubility in Mg, and together they form intermetallic precipitates. The precipitates can dissolve or re-precipitate according to the applied heat treatments. Hence, the material is characterized by high tensile strength, good fatigue behaviour [29], as

well as a reduced corrosion rate in compared to more conventional Mg alloys [28]. The wires were produced by cold drawing with 0.5 mm diameter and were then annealed.

2.2. μLMWD system

A customized μLMWD system was employed throughout the study [27]. The system consisted of an automated laser welding station (Powerweld HL 124P from Trumpf, Ditzingen, Germany), a flash pumped Nd:YAG and a custom build wire feeding system, namely Lachesis. The laser source provided 120 W maximum average power with pulse durations (τ) in μs to ms regime and a maximum pulse repetition rate (*PRR*) at 300 Hz. The maximum pulse energy (E) and the maximum peak power (P_{peak}) were of 50 J and 5 kW respectively. The laser beam was transmitted through fiber delivery with 0.4 mm core diameter, which was then focused with 200 mm collimating and 150 mm focal lenses. The minimum spot diameter was 0.3 mm, which could be automatically regulated to up to 5 mm. Substrates were mounted on the positioning system that provided two linear and a rotational axis. The laser head could be moved along a third axis to maintain the focal point at the desired height. The wire feed rate (*WFR*) was regulated via a Labview interface, synchronising the laser emission at the start of each new layer. The system details are shown in Fig.1, whereas the main specifications are reported in Table 1.

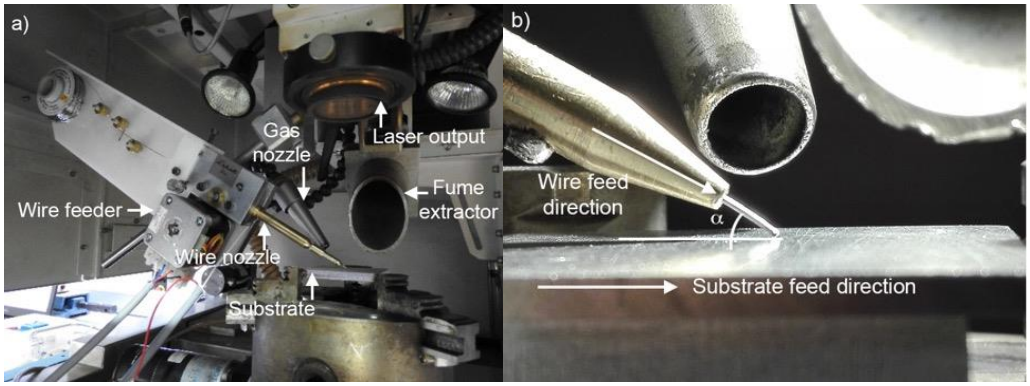

Fig. 1. Details of the μWLMD system. a) Processing zone showing the wire feeder assembly. b) Close up image of the deposition zone showing the wire and substrate feed directions.

Table 1. Main characteristics of the prototype μWLMD system.

Parameter	Value
Laser system	Trumpf PowerWeld HL 124P
Laser type	Flash pumped Nd:YAG
Emission wavelength (λ)	1064 nm
Max average power (P_{avg})	120 W
Max peak power (P_{pk})	5 kW
Max pulse energy (E)	50 J
Pulse duration (τ)	0.3-20 ms
Pulse repetition rate (*PRR*)	1-300 Hz
Beam parameter product (*BPP*)	16 mm·mrad
Min. beam diameter (d_0)	300 μm
Maximum wire feed rate (*WFR*)	900 mm/min
Wire diameter (d_w)	0.3-0.5 mm

2.3. Characterization

Surface morphology of the deposits was investigated with focus variation microscopy (Infinite Focus, Alicona, Graz, Austria). Images were acquired with 5X magnification with 1 μm lateral and 4 μm vertical estimated resolutions. Transversal cross-sections of single-tracks were made by abrasive saw cutting and abrasive paper polishing. Samples were later etched to reveal microstructure with a solution of 90 mL ethanol, 10 mL HNO_3. Optical

microscopy images were taken to measure the geometrical attributes of the deposited tracks (Leitz Ergolux 200 from Leica, Wetzlar, Germany).

2.4. Experimental plan

Single track experiments were carried out after the determination of the feasibility window through preliminary tests not reported here for the sake of brevity. Front feeding with a 30° feeding angle was conveniently adopted from previous studies. Stable processing conditions were realized with a relatively low wire feed rate (*WFR*) at 128 mm/min and low pulse repetition rate (*PRR*) at 10 Hz. In order to allow for a full coverage of the wire, spot diameter (d_s) was chosen 60% larger than the wire diameter at 0.8 mm. Due to the low rigidity of the Mg alloy wire, transverse speed (v) could be varied between 50 and 70 mm/s. Within the feasibility window pulse energy (E) could be varied between 2 and 3 J, whereas pulse duration (τ) between 3 and 5 ms. Higher pulse energies and lower pulse duration resulted in complete material consumption due to evaporation. Lower pulse energies and higher pulse durations resulted in no adhesion of the deposited wire. Within this feasibility window A 2^3 factorial plan with central points were executed. Linear tracks of 10 mm length were produced. Corner points were replicated 3 times, whereas 6 replications were produced for the central point. The main geometrical characteristics of the deposited single-tracks height (h), and width (w) were measured as depicted in Fig. 2 to calculated the aspect ratio defined as h/w. Deposit area (A_d) was measured in order to evaluate the deposition efficiency calculated from:

$$\eta = \frac{A_d}{\frac{\pi}{4} {d_w}^2 \cdot WFR \cdot \frac{1}{v} N} \quad (1)$$

where d_w is the wire diameter, and N is the number of layers, which is equal to 1 throughout the study. The results were evaluated against fluence, which is defined as:

$$F = \frac{E \cdot PRR}{d_S \cdot v} \quad (2)$$

The effect of process properties on material's mechanical properties was evaluated through microhardness measurements. Six measurements were taken for each combination. Analysis of variance (ANOVA) was applied to the response variables with statistical significance level at 5%. Details of the experimental plan in single-layer deposition study is summarized in Table 2.

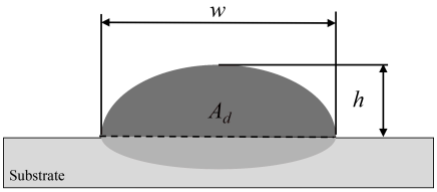

Fig. 2. Schematic description of the measured geometrical characteristics of the single-track deposits.

Table 2. Fixed and varied parameters in the study of single-layer depositions experiments.

Fixed parameters	**Level**		
Spot diameter, d_s (mm)	0.8		
Pulse repetition rate, PRR (Hz)	10		
Wire feeding angle, α (°)	30		
Wire feeding direction	Front		
Wire feed rate, WFR (mm/min)	128		
Shielding gas	Ar at 1.5 bar		
Varied parameters	**Levels**		
	Low	Mid	High
Pulse energy, E (J)	2	3	4
Pulse duration, τ (ms)	3	4	5
Transverse speed, v (mm/min)	50	60	70

3. Results

3.1. Single-track deposition geometry

Over the 30-run experimental plan only 3 deposits could not be realized, providing at least two replications for each parameter combination. In Fig.3, example 3D images of the single-track deposits are shown. The overall results show that the single tracks can be deposited without surface cracks. The surface morphology mainly consists of the overlapped molten tracks resulting from the pulsed emission profile of the laser. Fig.4 shows representative transveral cross-section images belonging to the different parameter combinations. Over the experimented range the deposit with (w) varied between approximately 450 and 915 μm, whereas the deposit height (h) was between 140 and 600 μm. It can be observed that very limited or partial dilution is present in the experimented region. Partial detachments are visible in the case of low pulse energy (E=2 J). This is expected to be due to a very limited amount of dilution in the process and a delamination caused by the mounting and polishing procedures. With the highest pulse energy (E=4 J), the deposits short, flat, and the penetration depth remains limited around 50 and 100 μm. Such profile change indicates a possible material loss, as the deposit area (A_d) is significantly reduced as well. In addition to a narrow feasibility window, the observed deposit morphologies confirm the low processability of the material under the laser beam. However, the dimensional range remains still within sub-milimetric range. On the other hand, the bioabsorbable Resoloy shows intact material structure without cracks despite the fast heating and cooling rates associated to the process.

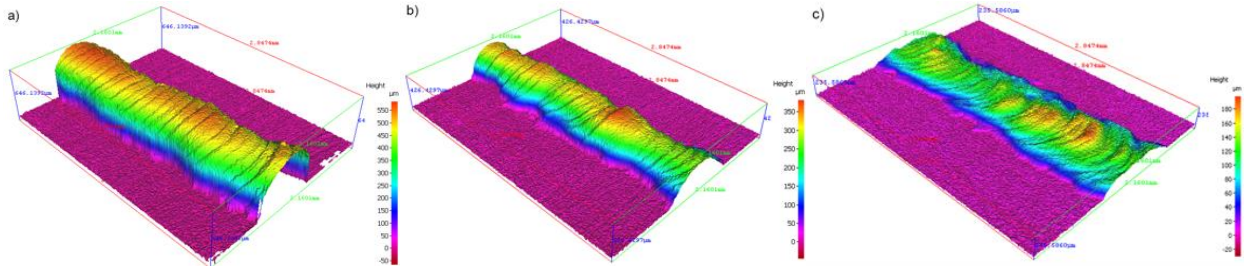

Fig. 3. Surface morphology of deposited single tracks. a) E=2 J; τ=3 ms; v=70 mm/min; b) E=3 J; τ=4 ms; v=60 mm/min; c) E=4 J; τ=5 ms; v=50 mm/min. Deposition direction is from right to left in the images

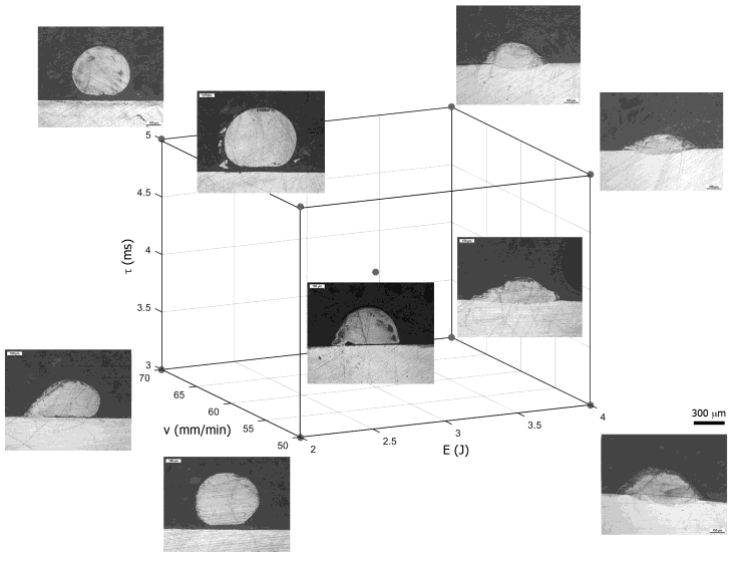

Fig. 4. Cross-section images of the single-layer depositions as function of process parameters.

Table 3 the results of ANOVA over aspect ratio *h*/*w* is reported, Fig. 5 shows the main effects plot of this response variable. As the ANOVA table confirms the only significant factor is the pulse energy (*E*), which generates a linear decreasing trend over the aspect ratio as it increases. As observed in the cross-section morphologies, with increases energy the deposits tend to become wider and shorter. Indeed, for micrometric applications control over both width and height is important. It should be considered that the minimum feature dimension will be constrained by the wire dimension. The laser beam will redistribute the fed wire volume over the deposited trajectory by melting causing a widening of the track with respect to the wire diameter [30]. The deposit height can be lower or higher, which depends on also the wire feed rate (*WFR*) and the energy input, which may generate material loss due to vaporization. Concerning also thin-walled structures, where the height of structure is expected to be much more than the width, the use of aspect ratio is adequate. Theoretically, the *h*/*w* aspect ratio can be 1 at maximum, in the absence of any flattening of the wire due to remelting and redistribution of the wire. The low energy content results in providing high aspect ratio values, appropriate for the thin-walled structure production. However, the same region corresponds to very low dilution zones, which appear to generate incomplete penetration zones. For multi-layered deposits, it should be noted that the successive deposited layers provide remelting of the previous ones. Hence, the use of low energy input can be beneficial after a first layer realized with high energy input allowing to adhere well to the substrate plate.

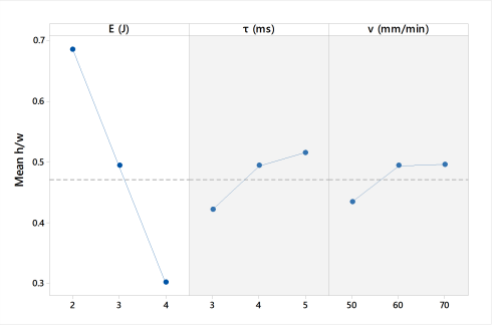

Fig. 5 Main effects plot for aspect ratio *h*/*w*. Insignificant parameters are shaded in grey.

Table 3. ANOVA table for single track aspect ratio (h/w).

Source	DF	Adj SS	Adj MS	F-Value	P-Value
Model	8	0.88543	0.110679	3.70	0.011
Linear	3	0.83191	0.277304	9.28	0.001
Pulse energy, E (J)	1	0.74412	0.74412	24.89	0.000
Pulse duration, τ (ms)	1	0.08889	0.08889	2.97	0.103
Transverse speed, v (mm/min)	1	0.01495	0.01495	0.50	0.489
2-way interactions	3	0.04934	0.016447	0.55	0.655
E*τ	1	0.02609	0.02609	0.87	0.363
E*v	1	0.01519	0.01519	0.51	0.486
τ*v	1	0.01042	0.01042	0.35	0.563
3-way interactions	1	0.00359	0.00359	0.12	0.733
E*τ*v	1	0.00359	0.00359	0.12	0.733
Curvature	1	0.00000	0.000003	0.00	0.992
Error	17	0.50825	0.029897		
Total	25	1.39369			
S= 0.17	R^2=63.5%		R^2_{adj}=46.4%		

3.2. Deposition efficiency

Besides determining the fraction of the material that is effectively deposited, the deposition efficiency is also an important indicator to whether the process is melting or vaporization dominant. A regression equation has fitted linking fluence to the measured deposition efficiency values, as expressed in the following equation.

$$\eta = 15.1/F\ (J/mm^2) \quad (3)$$

Table 4 reports the ANOVA table for the regression analysis, which confirm the model fits the data adequately with high R^2_{adj}, and without lack-of-fit. The model depicts a decay in the deposition efficiency as depicted in Fig. 6.

The only coefficient of the equation can be used as an indicator how processable is the material without excessive loss of vaporization. Compared to a previously studied material, AISI 301 stainless steel, the biodegradable Mg-alloy Resoloy shows around 46% lower overall efficiency ($\eta_{\text{AISI 301}}=21/F$ (J/mm^2)) [27].

Table 4. ANOVA table for the regression analysis for deposition efficiency (η).

Source	DF	Adj SS	Adj MS	F-Value	P-Value
Regression	1	5.58694	5.58694	282.75	0.000
Linear	1	5.58694	5.58694	282.75	0.000
1/F (J/mm^2)	26	0.51374	0.01976		
Error	4	0.01723	0.00431	0.19	0.941
Lack-of-fit	22	0.49651	0.02257		
Pure error	27	6.10068			
Total					
S= 0.14	R^2=91.6%		R^2_{adj}=91.3%		

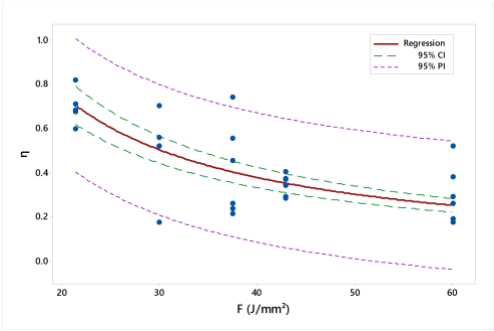

Fig. 6. Deposition efficiency as a function of fluence in the experimented region.

4. Conclusions

The present work demonstrates the single-track deposition of a biodegradable Mg-alloy with rare earth wires with a pulsed laser operating at ms pulse regime. The main aim of the work has been to identify the processability of this heat sensitive alloy and the possibility to achieve sub-milimetric process resolution for future use in biodegradable implant production by additive manufacturing. The main outcomes of the work are as follows.

- The biodegradable Mg-alloy possesses a narrow process window. This is mainly due its low melting and vaporization points. Despite the high sensitivity to the energy input, the deposits were crack and pore free.
- Within the processing window, the main influential parameter is the pulse energy, which can vary the aspect ratio *h*/*w* between 0.3 and 0.7 in average. The achieved single layers were in micrometric range both in terms of width and height confirming the feasibility of the process.
- The processability of the biodegradable Mg-alloy is compared to a highly processable austenitic AISI 301 steel. The biodegradable Mg-alloy shows lower overall deposition efficiency. These are mainly due to the low melting and vaporization points of the Mg-alloy as well as its high conductivity.

The results underline the delicate processing conditions required for the Mg-alloys also with the wire feedstock. Multiple-layer deposition conditions should be further investigated to evaluate the heat accumulation between consecutive layers and its effect on the material properties as well as the deposit geometry.

Acknowledgements

The author wishes to express his gratitude to Francesco Buffo and Matteo Colopi for their contribution to the experimental work. Fort Wayne Metals are acknowledged for their support. This work was supported by Regione Lombardia under within project MADE4LO under the call "POR FESR 2014-2020 ASSE I - AZIONE I.1.B.1.3".

References

[1] F. Witte, Acta Biomater. 6 (2010) 1680–92.
[2] P. Zartner, R. Cesnjevar, H. Singer, M. Weyand, Catheter. Cardiovasc. Interv. 66 (2005) 590–4.
[3] A.G. Demir, B. Previtali, Q. Ge, M. Vedani, W. Wu, F. Migliavacca, L. Petrini, C.A. Biffi, M. Bestetti, Int. J. Comput. Integr. Manuf. 27 (2014) 936–945.
[4] M.P. Staiger, A.M. Pietak, J. Huadmai, G. Dias, Biomaterials 27 (2006) 1728–34.
[5] S. Farè, Q. Ge, M. Vedani, G. Vimercati, D. Gastaldi, F. Migliavacca, L. Petrini, S. Trasatti, Matéria (Rio Janeiro) 15 (2010) 96–103.
[6] L. Wang, G. Fang, L. Qian, S. Lee, J. Duszczyk, J. Zhou, Prog. Nat. Sci. Mater. Int. 24 (2014) 500–506.
[7] S. Nayak, B. Bhushan, R. Jayaganthan, P. Gopinath, J. Mech. Behav. Biomed. Mater. 59 (2016) 57–70.
[8] A.G. Demir, B. Previtali, C.A. Biffi, Adv. Mater. Sci. Eng. 2013 (2013).
[9] A.G. Demir, B. Previtali, Biointerphases 9 (2014) 29004.
[10] M. Harooni, B. Carlson, in:, ICALEO 2013, 2013, pp. 509–519.
[11] D. Min, J. Shen, S. Lai, J. Chen, N. Xu, H. Liu, Opt. Lasers Eng. 49 (2011) 89–96.
[12] B.Y.L.E.M. Urr, S.M.G. Aytan, F.M. Edina, H.L. Opez, (2010) 1999–2032.
[13] B. Vandenbroucke, J.-P. Kruth, Rapid Prototyp. J. 13 (2007) 196–203.
[14] D.D. Gu, W. Meiners, K. Wissenbach, R. Poprawe, Int. Mater. Rev. 57 (2012) 133–164.
[15] A.G. Demir, B. Previtali, Mater. Des. 119 (2017) 338–350.
[16] D. Ding, Z. Pan, D. Cuiuri, H. Li, Int. J. Adv. Manuf. Technol. 81 (2015) 465–481.
[17] W.U.H. Syed, A.J. Pinkerton, L. Li, Appl. Surf. Sci. 247 (2005) 268–276.
[18] J. Lin, Opt. Laser Technol. 31 (1999) 233–238.
[19] F. Martina, J. Mehnen, S.W. Williams, P. Colegrove, F. Wang, J. Mater. Process. Technol. 212 (2012) 1377–1386.
[20] J.D. Kim, K.H. Kang, J.N. Kim, Appl. Phys. A 79 (2004) 1583–1585.
[21] J. Do Kim, Y. Peng, J. Mater. Process. Technol. 104 (2000) 284–293.
[22] J. Do Kim, Y. Peng, Opt. Lasers Eng. 33 (2000) 299–309.
[23] N.I.S. Hussein, J. Segal, D.G. McCartney, I.R. Pashby, Mater. Sci. Eng. A 497 (2008) 260–269.
[24] S. Jhavar, N.K. Jain, C.P. Paul, J. Mater. Process. Technol. 214 (2014) 1102–1110.
[25] E. Capello, D. Colombo, B. Previtali, J. Mater. Process. Technol. 164–165 (2005) 990–1000.
[26] E. Capello, B. Previtali, J. Mater. Process. Technol. 174 (2006) 223–232.
[27] A.G. Demir, Opt. Lasers Eng. 100 (2018).
[28] M. Stekker, N. Hort, F. Feyerabend, E. Hoffman, M. Hoffman, R. Horres, (2016) 1–31.
[29] J.E. Griebel A.J., Schaffer, Fatigue Performance of Resoloy® Magnesium Alloy Wire, 2016.
[30] T.E. Abioye, J. Folkes, A.T. Clare, J. Mater. Process. Technol. 213 (2013) 2145–2151.